A Combined DSC, X-Ray Diffraction, and Molecular Modelling Study of Chiral Discrimination in the Purification of Enantiomeric Mixtures of *cis*-Permethrinic Acid†

Ferenc Faigl,[a,*] Kálmán Simon,[b] Antal Lopata,[c] Éva Kozsda,[b] Richárd Hargitai,[c] Mátyás Czugler,[d] Mária Ács,[e] and Elemér Fogassy[e]

[a] *Research Group for Organic Chemical Technology, Hungarian Academy of Sciences, P.O.B. 91, Budapest H-1521, Hungary*

[b] *CHINOIN Pharmaceutical and Chemical Works Ltd., P.O.B. 110, Budapest H-1325, Hungary*

[c] *CheMicro Ltd., Budapest, Salamon u. 13/a, H-1105, Hungary*

[d] *Central Research Institute for Chemistry, Hungarian Academy of Sciences, P.O.B. 17, Budapest H-1525, Hungary*

[e] *Department of Organic Chemical Technology, Technical University, P.O.B. 91, Budapest H-1521, Hungary*

Purification of the non-racemic enantiomeric mixtures of *cis*-permethrinic acid has been performed by selective precipitation of the diastereoisomeric homo- (RCPAC) and hetero- (RSCPAC) dimers of the acid. The differences between the properties of the dimers have been studied using DSC and *X*-ray diffraction measurements. Molecular mechanics and quantum chemical calculations have been performed in order to describe quantitatively the energy differences and intermolecular interactions formed and to shed light on the mechanism of chiral discrimination in the separation of *cis*-permethrinic acid isomers.

Although the dimer-forming affinity and ability of carboxylic acids are well-known‡ this fact is especially important in the case of chiral acids. Since the mid 1970s, only a few papers dealing with chiral associates have been published. Horeau described the non-equivalence of the enantiomer purity and optical purity in solution of some optically impure α-substituted succinic acids[1] and n.m.r. studies were undertaken showing the associate-forming ability of chiral phosphoric acids[2] and the above mentioned succinic acid derivatives.[1] The presence of enantiomer associates can even influence the direction of a chemical reaction,[3] but the detection of these associates under the condition of selective precipitation has not yet been solved.

As the associate formation must precede the precipitation, most of the characteristic features of the second-order interactions in the associates can also be found in the solid state. Jacques and co-workers[4] have studied the thermal behaviour of racemic and optically active crystals. They found that the stability of the racemic compound is approximately proportional to the difference between the melting point of the racemate and the enantiomer.[4] Given a chiral molecule, it should be possible to determine by a calculation of the packing mode the energy difference between the racemic and enantiomeric crystals and to find the intermolecular interactions which stabilize the hetero- and homo-associates. The difference in the stability of hetero- and homo-associates could result in the selective reactions of the enantiomeric mixtures. Thus, it is worth comparing the crystal structure, the thermal behaviour and the chemical properties of a given racemate and one of its optically active isomers. However, so far as we are aware no investigation of this type has yet been carried out.

As a model compound we have chosen *cis*-2,2-dimethyl-3-(2,2-dichlorovinyl)cyclopropanecarboxylic acid (*cis*-permethrinic acid), an intermediate of the well-known insecticides 'Permethrin' and 'Cypermethrin'.[5] A number of papers deal with the optical resolution of the racemic acid.[6,7] In most cases partial resolution can only be achieved and the obtained enantiomeric mixtures must be purified. Therefore the *cis*-permethrinic acid seemed to be a proper model for our studies.

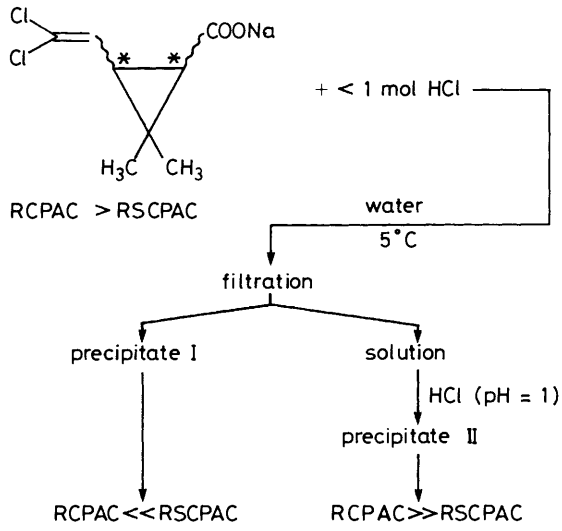

Scheme. Selective precipitation of non-racemic enantiometric mixtures of *cis*-permethrinic acid.

Results and Discussion

Chemical and Thermal Behaviour.—When an aqueous solution of the sodium salt of the optically impure *cis*-permethrinic acid is treated with a non-equivalent amount of hydrochloric acid, the optical purity of the free acid precipitated and that of the sodium salt in solution differ from the optical purity of the starting sample (see the Scheme).

† *cis*-2,2-Dimethyl-3-(2,2-dichlorovinyl)cyclopropanecarboxylic acid.

‡ For acetic acid: L. Barcza and K. Mihályi, *Z. Phys. Chem.* (*Munnich*), 1977, **104**, 213. For benzoic acid: L. Barcza, Á. Buvári, and M. Vajda, *Z. Phys. Chem.* (*Munnich*), 1976, **102**, 35.

Table 1. Physicochemical parameters and crystal data.

	RSCPAC	RCPAC
Formula	$C_8H_{10}Cl_2O_2$	$C_8H_{10}Cl_2O_2$
M	209.3	209.3
Melting point/°C	87.2	90.5
Heat of fusion/kJ mol^{-1}	22.36	13.61
a/Å	6.017(1)	6.634(2)
b/Å	7.800(1)	8.031(2)
c/Å	11.264(2)	18.947(4)
α/°	81.12(2)	
β/°	88.80(2)	90.42(2)
γ/°	70.28(2)	
V/Å^3	491.0	1 003.4
Space group	$P\bar{1}$ triclinic	$P2_1$ monoclinic
Z	2	4
D g cm^{-3}	1.413	1.384
μ(Cu-K_α)/cm^{-1}	57.5	56.0
Crystal size/mm	0.20 × 0.22 × 0.25	0.06 × 0.13 × 0.20
θ_{max}/°	75	75
No. of independent reflections	2 024	2 225
Decay (%)	slight (5%)	31
Intensities used	1 893 [$I > 3\sigma(I)$]	1 227 [$I > 2\sigma(I)$]
R	0.067	0.070
R_w	0.103	0.062
p	0.01	0.01

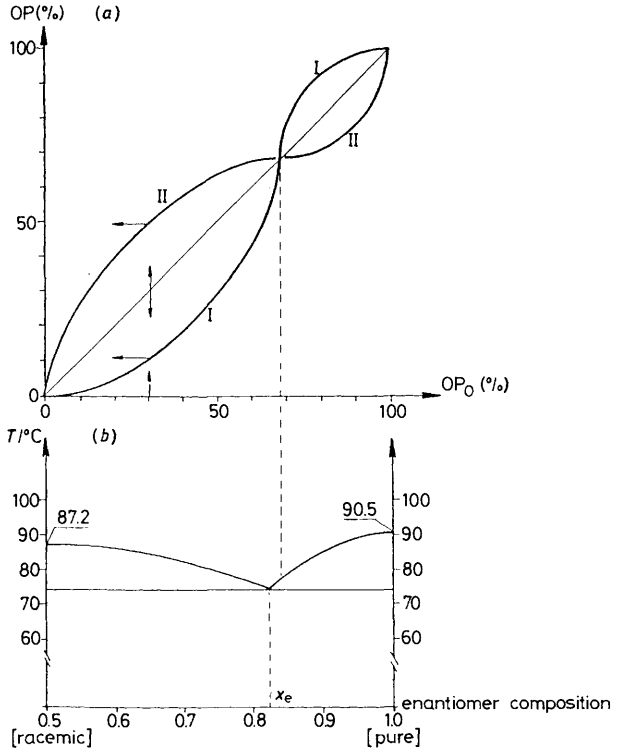

Figure 1. (*a*) Change in optical purity (OP) of the precipitated acid (curve I) and of the unchanged sodium salt remaining in solution (curve II) as a function of the initial optical purity (OP_0), in the course of selective precipitation of *cis*-permethrinic acid. (*b*) Binary phase diagram of *cis*-permethrinic acid isomers.

This phenomenon was systematically investigated. The enantiomer compositions of the initial samples were gradually changed, and the optical purity of the liberated acid [curve I in Figure 1(*a*)] and that of the salt remaining in solution (curve II) were measured. The values obtained are plotted against the initial optical purity (OP_0) in Figure 1(*a*). There are intersection points at the optically pure and at the racemic composition; furthermore, there is an inflection point at *ca.* 70%. Below the initial opitical purity of 70% the heterodimer (RSCPAC) is more abundant in the precipitate. Above this initial optical purity the difference in solubility between the diastereoisomer dimers is overcompensated by the higher concentration of the optically active homodimers. This intersection point corresponds to the eutectic composition of the binary phase diagram [x_e in Figure 1(*b*), thermal data are shown in Table 1]. The curve II has an inverted shape related to curve I, (the inflection points coincide with that of the intersection). The slopes of the curves depend on the amount of the achiral agent applied for obtaining the first portion. The selectivity of the method shows the difference in chemical properties between the enantiomeric and racemic forms. In our experiments the most effective separation has been achieved when the initial optical purity is *ca.* 30%. In this case the optical purity of the first fraction is *ca.* 10%, so the ratio of RSCPAC dimer to RCPAC dimer is 9:1. The optical purity of the *cis*-permethrinic acid sodium salt remaining in solution is *ca.* 50% (RSCPAC:RCPAC dimer ratio is 1:1).

A comparison of the thermal data for RSCPAC and RCPAC has not correctly explained the large selectivity in the above chemical reaction. The melting point of RCPAC is higher than that of RSCPAC but the difference is small (3.3 °C) and the heat of fusion of RSCPAC is larger than that of RCPAC (Table 1). The free energy of formation (calculated by the method of Jacques)[4] also showed the racemic form of *cis*-permethrinic acid to be more stable by 0.61 kcal mol^{-1}.

X-Ray Investigations.—Packing arrangements. The crystals of both the racemic (RSCPAC) and the enantiomeric form (RCPAC) of *cis*-permethrinic acid are built up from dimers. Dimers are linked by hydrogen bridges formed between the carboxy groups (Figure 2 and Table 2). RSCPAC has a (crystallographic) centre of symmetry and the unit cell is composed of two mirror image molecules, while in the optically

Table 2. Hydrogen bonds, second-order interactions[a] and their energies in RSCPAC and RCPAC.[b]

Atoms	Symmetry	H···A/Å	D–H···A/°	U_N[c]	U_C[d]
RSCPAC					
O(1)–H(10)···O(1)	$[-x, 1-y, 1-z]$	1.76	164	−5.159	−5.763
C(5)–H(51)···O(1)	$[-x, 2-y, 1-z]$	2.75	149	−0.002	−0.173
C(5)–H(53)···Cl(2)	$[x, y+1, z]$	3.02	164	−0.052	−0.053
C(7)–H(7)···Cl(1)	$[x-1, y, z]$	2.95	157	−0.047	−0.567
RCPAC					
O(1)–H(10)···O(2)*	$[x, y, z]$	1.70	151	−5.775	−5.843
O(1)*–H(10)*···O(2)	$[x, y, z]$	1.66	169	−5.916	−5.785
C(1)–H(1)···O(1)*	$[x+1, y, z]$	2.56	142	0.156	−1.077
C(1)*–H(1)*···O(1)	$[x-1, y, z]$	2.63	158	0.082	−1.136
C(5)–H(5)···O(2)	$[x+1, y, z]$	2.67	157	0.021	−0.331
C(6)–H(6)···Cl(1)	$[x, y+1, z]$	2.94	147	−0.047	−0.305
O(1)–H(10)···Cl(1)*	$[-x, y-0.5, 1-z]$	2.94	111	−0.066	−1.298

[a] Intermolecular contacts, shorter than the sum of the van der Waals radii of the atoms involved. [b] The asterisk indicates atoms of RCPAC2. [c] U_N: energy of non-bonded interactions/kcal mol^{-1}. [d] U_C: energy of Coulomb interactions/kcal mol^{-1}.

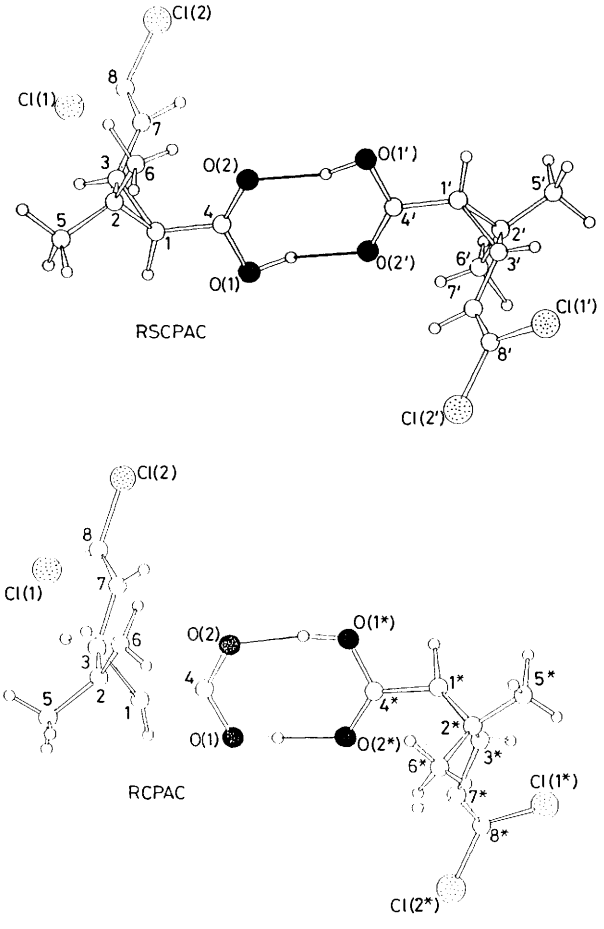

Figure 2. Dimers of racemic (RSCPAC) and optically active (RCPAC) *cis*-permethrinic acid.

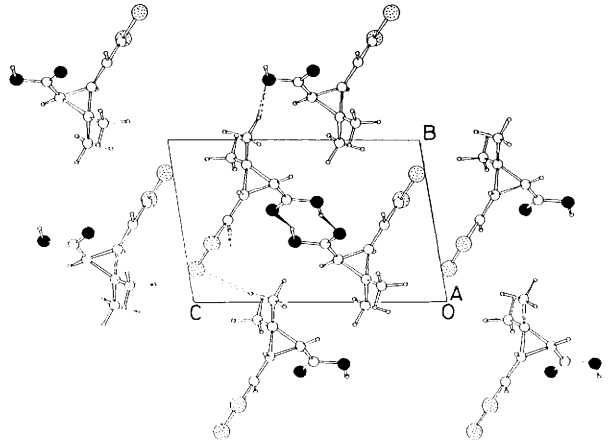

Figure 3. The packing arrangement of the racemic *cis*-permethrinic acid (RSCPAC) viewed along the *a* axis. Hydrogen bonds and short second-order interactions are indicated by heavy continuous (——) and thin dotted lines (– – –), respectively.

active crystals (RCPAC) the dimers are formed by two crystallographically independent molecules (RCPAC1 and RCPAC2). Crystal data are listed in Table 1.

Conformation and geometry. In the optically active crystal (RCPAC) the cyclopropane rings are parallel, while the carboxy and dichlorovinyl groups are orthogonal to the *bc* plane. In RCPAC1 the C=C double bond of the vinyl group points in the direction of the *b* axis, while in RCPAC2 it is directed along the *c* axis. Dimers composed by homochiral acids show a sickle shape when projected along the *a* axis. This sickle is composed of the dichlorovinyl, cyclopropane and carboxy groups. The axes of these sickles are oriented in the *bc* plane, in such a way that the crystallographic twofold screw axis enables them to adopt a perpendicular arrangement.

In the racemic crystal (RSCPAC) the cyclopropane ring is parallel to the *bc* plane. The heterodimer shows an 'S' shape (viewed along the *a* axis). A symmetry centre and the translational symmetry adopts a parallel arrangement of the S-forms. A comparison of the crystal structures of RCPAC and RSCPAC shows that the heterodimer is more compact. Crystals are built up from the relatively rigid dimer conformers with second-order interactions. The second-order interactions are indicated by a dotted line on the packing arrangements (Figures 3 and 4). The number of the weak second-order interactions (where the interatomic distances are shorter than the sum of the van der Waals radii of the atoms involved) are only slightly different in the crystals (2 × 3 in the racemate, and 5 in the enantiomer, see Table 2), in accordance with the relatively low difference in their thermal data (Table 1).

The X-ray measurements thus result only in qualitative

Table 3. The CNDO/2 net atomic charges and the total energies of the separate molecules RCPAC1, RCPAC2, RSCPAC1, and RSCPAC2.

	RCPAC1		RCPAC2		RSCPAC1 and RSCPAC2	
Atom	Total	Net	Total	Net	Total	Net
C(1)	4.0985	−0.0985	4.1086	−0.1086	4.0638	−0.0638
C(2)	3.8915	0.1085	3.8902	0.1098	3.9148	0.0852
C(3)	4.0042	−0.0042	4.0021	−0.0021	3.9733	0.0267
C(4)	3.5919	0.4081	3.5907	0.4093	3.5970	0.4030
C(5)	4.0488	−0.0488	4.0570	−0.0570	4.0155	−0.0155
C(6)	4.0615	−0.0615	4.0589	−0.0589	4.0345	−0.0345
C(7)	3.9519	0.0481	3.9549	0.0451	3.9771	0.0229
C(8)	3.9132	0.0868	3.9082	0.0918	3.9056	0.0944
O(1)	6.2746	−0.2746	6.2769	−0.2769	6.2673	−0.2673
O(2)	6.3507	−0.3507	6.3635	−0.3635	6.3503	−0.3503
Cl(1)	7.1407	−0.1407	7.1401	−0.1401	7.1457	−0.1457
Cl(2)	7.1224	−0.1224	7.1230	−0.1230	7.1275	−0.1275
H(1)	0.9401	0.0599	0.9348	0.0652	0.9706	0.0294
H(3)	0.9503	0.0497	0.9507	0.0493	0.9658	0.0342
H(51)	0.9706	0.0294	0.9771	0.0229	0.9893	0.0107
H(52)	0.9849	0.0151	0.9840	0.0160	0.9986	0.0014
H(53)	0.9879	0.0121	0.9709	0.0291	0.9924	0.0076
H(61)	0.9774	0.0226	0.9651	0.0349	0.9640	0.0360
H(62)	0.9787	0.0213	0.9703	0.0297	0.9948	0.0052
H(63)	0.9618	0.0382	0.9793	0.0207	0.9949	0.0051
H(7)	0.9624	0.0376	0.9577	0.0423	0.9311	0.0689
H(10)	0.8359	0.1641	0.8359	0.1641	0.8261	0.1739
Energy/ kcal mol^{-1}	−83 522		−83 533		−83 707	

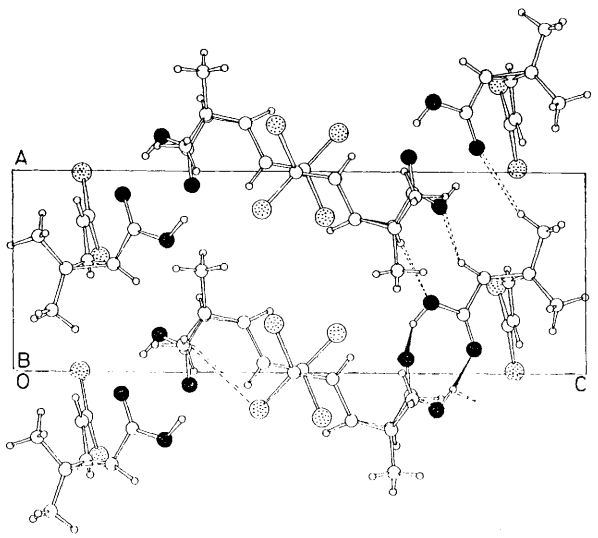

Figure 4. The packing arrangement of the optically active *cis*-permethrinic acid (RCPAC) viewed along the *b* axis. Hydrogen bonds and the short second-order interactions are indicated by heavy continuous (——) and thin dotted lines (– – –), respectively.

pictures of the energy differences between the dimers. We therefore performed molecular mechanics and quantum chemical calculations on the RSCPAC and RCPAC dimers in order to describe quantitatively the above energy differences and the intermolecular interactions formed.

Molecular Modelling Investigations.—Starting from the molecular geometries determined by single-crystal X-ray diffraction measurements, CNDO/2 calculations were carried out on separate RCPAC and RSCPAC molecules. The CNDO/2 net atomic charges and the total energies of RCPAC1, RCPAC2, and RSCPAC (the values of RSCPAC1 are equal to those of RSCPAC2) are summarized in Table 3. The same geometries and net atomic charges were used in the molecular mechanics calculations on the RCPAC and RSCPAC dimers. Non-bonded (van der Waals and hydrogen bonding) interactions were taken into account using Lennard–Jones 6–12 and general hydrogen bond 10–12 potential functions. The energy parameters used in these functions were those of Némethy, Pottie, and Scheraga.[8] In addition, Coulomb interactions were also considered using the CNDO/2 net atomic charges.

The molecular mechanics calculations on the RCPAC and RSCPAC dimers resulted in the potential energy contributions shown in the upper line of Table 4. Contrary to our expectations the homodimer turned out to be more stable than the heterodimer when we considered only the single dimers. The question arises as to how this stability order might be changed by consideration of the crystal packing. To answer this question we carried out the above molecular mechanics calculations using the so-called crystal space option, *i.e.*, we considered the intermolecular interactions of RCPAC1 and RSCPAC1 molecules with all the molecules in their unit cell and in 6 or 26 neighbouring unit cells as well [in the direction of the faces(6), or the faces(6), the edges(12) and the vertices(8) of the unit cell, respectively]. Since the unit cell of RCPAC contains four molecules (two dimers) whereas the unit cell of RSCPAC contains two molecules (one dimer) the energy values calculated for RCPAC1 were normalized to relate them to the same number of molecules. These interaction energies are described in the central and bottom lines of Table 4. It can be seen that the consideration of the crystal packing (27 unit cells) shows the heterodimer to be more stable than the homodimer and this is in good accordance with the chemical observation. In RSCPAC the compact arrangement results in large attractive van der Waals interactions while the sum of the energy contributions of Coulomb interactions results in a little repulsion. In RCPAC both types of interactions are attractive.

The next question is: what kind of atom–atom interactions stabilize the crystals of the RCPAC and RSCPAC dimers? In

Table 4. Calculated energies of the intermolecular interactions in the single dimers and in the case of 7 and 27 unit cells.

	RSCPAC			RCPAC		
	U_N[a]	U_C[b]	U[c]	U_N[a]	U_C[b]	U[c]
Dimer	−10.193	−0.795	−10.988	−11.311	−1.069	−12.380
7 unit cells	−26.584	0.112	−26.472	−19.627	−0.525	−20.152
27 unit cells	−35.116	5.102	−30.014	−23.296	−3.806	−27.102

[a] U_N/kcal mol^{-1}: energy of non-bonded interactions. [b] U_C/kcal mol^{-1}: energy of Coulomb interactions. [c] U/kcal mol^{-1}: total energy.

Table 5. Some examples of the distant intermolecular interactions (< 10 Å) in RSCPAC and RCPAC crystals.

Atoms	Cell	D···A/Å	U_N/kcal mol^{-1}	U_C/kcal mol^{-1}
RSCPAC				
C(4)···Cl(1)	[−1 0 0]	4.659	−0.035	−2.100
O(2)···C(2)	[−1 0 0]	4.603	−0.034	−1.080
O(2)···C(8)	[−1 0 0]	4.470	−0.048	−1.233
C(7)*···Cl(2)	[1 0 1]	3.655	−0.102	−0.133
C(4)*···O(1)	[0 1 0]	5.441	−0.014	−3.299
C(4)*···O(2)	[0 1 0]	5.850	−0.013	−4.021
C(4)*···O(2)	[0 0 1]	9.279	−0.001	−2.535
C(4)*···Cl(2)	[0 0 1]	6.658	−0.004	−1.286
RCPAC				
O(2)···C(1)	[−1 0 0]	4.535	−0.037	−1.398
C(4)···O(2)	[1 0 0]	5.489	−0.018	−4.344
C(8)···O(2)	[0 −1 0]	4.417	−0.052	−1.148
C(4)···Cl(1)	[0 1 0]	3.378	−0.103	−2.832
C(8)*···O(2)	[0 −1 0]	4.002	−0.084	−1.313
Cl(2)*···C(4)	[0 −1 0]	3.778	−0.092	−2.210
Cl(1)*···C(4)	[1 −1 0]	4.274	−0.054	−2.245

U_N: energy of non-bonded interactions. U_C: energy of Coulomb interactions.

Table 2 are summarized the calculated energy contributions for the D–H···A interactions obtained from X-ray diffraction measurements in the usual way (the interatomic distances are shorter than the sum of the van der Waals radii of the atoms involved). The average energy of the O(1)–H···O(2) type contacts in the RCPAC dimer is −11.658 kcal mol^{-1}, while in the RSCPAC dimer it is −10.922 kcal mol^{-1}, and the D–H···A distances are shorter in the RCPAC dimer. The single homodimer is therefore more stable than the heterodimer. The other interactions, listed in Table 2, are rather weak. These contacts have not, therefore, explained the stability of the racemic form. We have found several stronger interactions between distant atoms in which the interatomic distances were higher than the sum of the van der Waals radii of the atoms involved. Some of the more attractive interactions are summarized in Table 5. The atoms which are mainly involved in these interactions are as follows: C(4), O(1), O(2), Cl(1), Cl(2), and sometimes C(1), C(2), C(7), and C(8). Coulomb interactions (U_C) between the partially charged positive and negative atoms are important (see Table 3) but the energies of the non-bonded interactions (U_N) between distant atoms and the energies of the shorter interactions (shown in Table 2) are of the same order.

The total energy of the distant interactions in the RSCPAC crystal is higher than that in the RCPAC crystal and the difference between the energies of hydrogen bonds is over-compensated. The majority of the distant contacts point in the direction of the *a*, *b* and *c* axes. This explains why we have found RSCPAC to be more stable than RCPAC when considering only six neighbouring unit cells in the crystal space option (see the centre line in Table 4).

The formation of this type of associate (in solution) must precede the precipitation in the course of selective precipitation of *cis*-permethrinic acid, and the energy differences revealed by our calculations are responsible for chiral discrimination in the above-mentioned process.

Conclusion

Studies on the chemical and thermal behaviour and the crystal structure of racemic and optically active *cis*-permethrinic acid showed only slight differences between the thermal behaviour of RSCPAC and RCPAC, and the hydrogen-bonding system was nearly identical in both structures. Nevertheless, selective reactions of non-racemic enantiomeric mixtures were observed. In order to explain quantitatively this phenomenon, molecular-modelling investigations were performed. Molecular mechanics calculations on the separate dimers showed the RCPAC dimer to be more stable than the RSCPAC dimer. Consideration of the crystal packing (*i.e.* all the molecules in 6 or 26 neighbouring unit cells), however, changed the stability order. This is in agreement with the experimental findings that RSCPAC crystallizes in the first step and that the stability of RSCPAC is higher than that of the RCPAC crystal. The results also showed that quite strong interactions may be formed between distant atoms and that these contacts play an important role in chiral discrimination in the course of selective precipitation. Therefore it is not appropriate to simply consider only those atoms which are closer to each other than the sum of their van der Waals radii in such interactions.

Experimental

Thermal data were recorded using the DSC Cell of the DUPONT 1090 TA-SYSTEM. The optical rotations were measured by a Perkin Elmer 241 polarimeter.

Table 6. Fractional co-ordinates of RSCPAC; esds are in parentheses.

Atom	*x/a*	*y/b*	*z/c*
Cl(1)	0.865 6(1)	0.367 7(1)	0.889 55(8)
Cl(2)	0.514 2(1)	0.207 27(9)	0.971 68(7)
O(1)	0.208 6(3)	0.622 8(3)	0.445 2(1)
O(2)	0.043 6(3)	0.577 3(3)	0.619 9(1)
C(1)	0.330 4(4)	0.731 1(3)	0.603 7(2)
C(2)	0.261 5(4)	0.852 2(3)	0.700 8(2)
C(3)	0.449 3(4)	0.666 3(3)	0.730 2(2)
C(4)	0.179 7(4)	0.636 8(3)	0.560 3(2)
C(5)	0.346 6(5)	1.015 5(4)	0.682 6(3)
C(6)	0.023 8(5)	0.891 9(4)	0.757 4(3)
C(7)	0.411 1(4)	0.513 5(3)	0.809 9(2)
C(8)	0.575 7(4)	0.381 6(3)	0.879 4(2)

Table 7. Fractional co-ordinates for RCPAC1 and RCPAC2; esds are in parentheses.

Atom	*x/a*	*y/b*	*z/c*
RCPAC1			
Cl(1)	0.440 3(4)	−0.289 5(0)	0.848 2(1)
Cl(2)	0.021 1(3)	−0.254 8(3)	0.880 8(1)
O(1)	0.353 4(7)	0.409 5(8)	0.732 7(2)
O(2)	0.125 0(7)	0.321 1(8)	0.808 9(2)
C(1)	0.478(1)	0.254(1)	0.825 6(3)
C(2)	0.507(1)	0.255(1)	0.905 7(3)
C(3)	0.464(1)	0.095(1)	0.869 2(4)
C(4)	0.299(1)	0.330(1)	0.790 1(3)
C(5)	0.716(1)	0.279(1)	0.929 9(4)
C(6)	0.352(1)	0.330(1)	0.954 1(4)
C(7)	0.272(1)	0.004(1)	0.876 6(4)
C(8)	0.247(1)	−0.157(1)	0.869 0(4)
RCPAC2			
Cl(1)	−0.193 9(4)	0.786 5(6)	0.431 6(1)
Cl(2)	0.229 1(3)	0.808 1(4)	0.457 5(1)
O(1)	−0.169 9(8)	0.480 2(9)	0.742 6(3)
O(2)	0.074 5(7)	0.617 6(8)	0.690 1(2)
C(1)	−0.272(1)	0.681(1)	0.662 3(4)
C(2)	−0.280(1)	0.876(1)	0.663 8(4)
C(3)	−0.238(1)	0.785(1)	0.595 6(3)
C(4)	−0.106(1)	0.592(1)	0.697 3(4)
C(5)	−0.489(1)	0.945(1)	0.669 6(4)
C(6)	−0.121(1)	0.976(1)	0.701 3(4)
C(7)	−0.038(1)	0.795(1)	0.560 8(4)
C(8)	−0.007(1)	0.797(1)	0.492 9(4)

Illustrative Example for the Selective Precipitation of cis-*Permethrinic Acid.*—1(*R*)-*cis*-permethrinic acid (10.45 g, 0.05 mol; optical purity 30%) was dissolved in aqueous sodium hydroxide (70 cm^3 containing 0.05 mol of sodium hydroxide). Hydrochloric acid (10 cm^3, 2 mol dm^{-3}) was added dropwise, at 5 °C, with stirring. The precipitate was filtered off (4.5 g; $[\alpha]_D^{22}$ 2.2°, *c* 1.0 in $CHCl_3$; optical purity 7%). The filtrate was acidified to pH 1 and the second crop of precipitate was filtered off (5.8 g; $[\alpha]_D^{22}$ 16°, *c* 1.0 in $CHCl_3$; optical purity 50%).

X-Ray Investigations.—Suitable crystals were grown from hexane. The single crystal investigation was performed on an Enraf-Nonius CAD4 diffractometer, using Cu–K_α radiation. The experimental conditions are given in Table 1. The observed decay was corrected by means of a systematic measurement of the intensity standard reflections. The structure was solved by routine application of the MULTAN-84 program. All hydrogen atoms were identified in Fourier difference maps. Positional and thermal parameters were not refined for the hydrogen atoms. The fractional co-ordinates with their esd values in parentheses are given in Tables 6 and 7. Bond lengths, bond angles and torsion angles are summarized in Table 8. Calculations were carried out on a PDP 11/34 minicomputer with the Enraf-Nonius SDP program package with local modifications. Thermal parameters, hydrogen atom co-ordinates and tables of observed and calculated struc-

Table 8. Bond lengths, bond angles and torsion angles with esd values in parentheses.

	RSCPAC	RCPAC1	RCPAC2
Bond lengths/Å			
Cl(1)–C(8)	1.716(4)	1.712(9)	1.695(9)
Cl(2)–C(8)	1.718(3)	1.709(9)	1.710(9)
O(1)–C(4)	1.321(3)	1.314(9)	1.312(11)
O(2)–C(4)	1.214(4)	1.213(9)	1.224(9)
C(1)–C(2)	1.515(4)	1.529(10)	1.564(15)
C(1)–C(3)	1.541(4)	1.519(13)	1.533(12)
C(1)–C(4)	1.477(5)	1.494(11)	1.472(12)
C(2)–C(3)	1.500(4)	1.487(13)	1.511(12)
C(2)–C(5)	1.511(5)	1.470(11)	1.501(12)
C(2)–C(6)	1.507(6)	1.505(12)	1.500(13)
C(3)–C(7)	1.458(4)	1.478(12)	1.493(11)
C(7)–C(8)	1.322(4)	1.315(15)	1.304(11)
Bond angles/°			
C(2)–C(1)–C(3)	58.8(4)	58.4(9)	58.4(10)
C(2)–C(1)–C(4)	124.0(5)	122.5(12)	120.4(13)
C(3)–C(1)–C(4)	120.5(5)	122.4(12)	121.7(13)
C(1)–C(2)–C(3)	61.5(4)	60.5(9)	59.8(10)
C(1)–C(2)–C(5)	114.5(5)	114.8(12)	113.6(13)
C(1)–C(2)–C(6)	121.4(5)	121.8(12)	121.5(13)
C(3)–C(2)–C(5)	115.9(5)	115.7(12)	114.5(13)
C(3)–C(2)–C(6)	120.8(5)	120.0(12)	122.2(13)
C(5)–C(2)–C(6)	113.3(5)	113.9(12)	114.5(13)
C(1)–C(3)–C(2)	59.8(4)	61.1(9)	61.8(10)
C(1)–C(3)–C(7)	120.6(5)	121.7(13)	121.9(13)
C(2)–C(3)–C(7)	122.7(5)	122.9(13)	121.4(13)
O(1)–C(4)–O(2)	122.1(5)	122.7(13)	120.7(14)
O(1)–C(4)–C(1)	111.8(5)	110.4(11)	112.6(13)
O(2)–C(4)–C(1)	126.1(5)	126.9(13)	126.6(14)
C(3)–C(7)–C(8)	125.2(5)	125.8(15)	125.6(15)
Cl(1)–C(8)–Cl(2)	113.4(3)	113.9(9)	113.7(10)
Cl(1)–C(8)–C(7)	124.5(5)	123.0(13)	123.8(14)
Cl(2)–C(8)–C(7)	122.1(5)	123.1(13)	122.5(14)
Torsion angles/°			
C(2)–C(1)–C(4)–O(1)	147.5(6)	139.2(14)	125.6(15)
C(2)–C(1)–C(4)–O(2)	−32.5(6)	−41.8(13)	−50.7(14)
C(3)–C(1)–C(4)–O(1)	−141.7(6)	−150.2(14)	−165.0(16)
C(3)–C(1)–C(4)–O(2)	38.3(5)	28.8(14)	18.7(14)
C(3)–C(7)–C(8)–Cl(1)	0.7(4)	−0.2(12)	−0.8(12)
C(3)–C(7)–C(8)–Cl(2)	179.5(7)	178.3(20)	179.9(21)
C(4)–C(1)–C(2)–C(3)	107.9(6)	110.7(15)	110.7(16)
C(4)–C(1)–C(3)–C(2)	−113.7(6)	−110.9(14)	−108.6(16)
C(5)–C(2)–C(1)–C(3)	107.4(5)	106.6(14)	105.6(15)
C(5)–C(2)–C(1)–C(4)	−144.7(6)	−142.7(14)	−143.7(15)
C(5)–C(2)–C(3)–C(1)	−105.1(6)	−105.2(14)	−104.1(15)
C(6)–C(2)–C(1)–C(3)	−110.5(6)	−109.0(15)	−111.4(16)
C(6)–C(2)–C(1)–C(4)	−2.7(5)	1.7(13)	−0.7(14)
C(6)–C(2)–C(3)–C(1)	111.5(6)	111.9(15)	110.4(16)
C(7)–C(3)–C(1)–C(2)	112.4(6)	112.9(16)	111.3(16)
C(7)–C(3)–C(1)–C(4)	−1.3(5)	2.0(13)	2.7(14)
C(7)–C(3)–C(2)–C(1)	−109.0(6)	−110.9(16)	−112.0(16)
C(7)–C(3)–C(2)–C(5)	145.9(6)	143.8(17)	143.9(17)
C(7)–C(3)–C(2)–C(6)	2.5(5)	0.9(14)	−1.7(14)
C(8)–C(7)–C(3)–C(1)	139.1(7)	132.7(19)	141.2(20)
C(8)–C(7)–C(3)–C(2)	−149.3(7)	−153.4(20)	−144.6(20)

ture factors are available from the authors upon request. CNDO/2 and molecular mechanics calculations were carried out using the molecular modelling package MOLIDEA[9] developed for IBM PC XT/AT computers.

Acknowledgements

The authors are grateful to Dr. G. H. Pokol, Institute of General and Applied Chemistry, Technical University, Budapest for the DSC investigations and to the CHINOIN Pharmaceutical and Chemical Works Ltd. for financial support.

References

1 A. Horeau and J. P. Guette, *Tetrahedron*, 1974, **31**, 1923.
2 M. I. Kabacnik, T. A. Mastrjukova, E. I. Fegyin, M. S. Vajsberg, L. L. Morozov, P. V. Petrovskij, and A. E. Sipov, *Tetrahedron*, 1976, **32**, 1719.
3 H. Wynberg and B. Feringa, *Tetrahedron*, 1976, **32**, 1831.
4 J. Jacques, A. Collet, and S. H. Wilen, 'Enantiomers, Racemates and Resolutions,' Wiley, New York, 1981, p. 100.
5 M. Elliott in 'Synthetic Pyrethroids,' *A.C.S. Symp. Ser. 42*, ed. M. Elliott, Washington D.C., 1977, p. 8.
6 E. Fogassy, F. Faigl, M. Ács, K. Simon, É. Kozsda, B. Podányi, M. Czugler, and G. Reck, *J. Chem. Soc., Perkin Trans. 2*, 1988, 1385.
7 (*a*) BRD Pat. Appl., No. 2 826 952/1980 (*Chem. Abstr.*, 1980, **93**, 7732u); (*b*) GB Pat. Appl., No. 2 008 589/1977 (*Chem. Abstr.*, 1980, **92**, 76735p); (*c*) Fr. Pat., No. 1 536 488/1979 (*Chem. Abstr.*, 1969, **71**, 90923w); (*d*) Eur. Pat. Appl., No. 119 463/1984 (*Chem. Abstr.*, 1985, **102**, 61849ç).
8 G. Némethy, M. S. Pottie, and H. A. Scheraga, *J. Phys. Chem.*, 1983, **47**, 1883.
9 A. Lopata, Z. Gabányi, Á. Bencze, and D. Fodor, MOLIDEA Version 2.20, Released July 1, 1989, CheMicro Ltd. Salamon u. 13/a, Budapest, H-1105, Hungary.

Paper 9/00556K
Received 6*th February* 1989
Accepted 18*th July* 1989